Radiation-Induced Catalysis on Oxide Surfaces: Degradation of Hexachlorobenzene on γ-Irradiated Alumina Nanoparticles

George Adam Zacheis,[†] Kimberly A. Gray,*[,†] and Prashant V. Kamat*[,‡]

Department of Civil Engineering, 2145 Sheridan Road, Northwestern University, Evanston Illinois 60208-3109 and Notre Dame Radiation Laboratory, University of Notre Dame, Notre Dame, Indiana 46556-0579

Received: January 18, 1999

There is a need to understand fundamentally the radiolytic processes occurring on metal oxide surfaces, processes which may determine the fate of pollutants in high level nuclear storage tanks and may also be used to remediate contaminated materials, such as soils. Radiation-induced, surface chemical processes on alumina (Al_2O_3) were studied to determine if the phenomena of charge separation and subsequent charge-transfer resulted in the catalytic degradation of an adsorbed compound, hexachlorobenzene (HCB). Radiolytic transformation of HCB adsorbed to alumina and potassium bromide (KBr) was monitored by a suite of analytical methods including diffuse reflectance, UV, and Fourier transform infrared spectroscopy (FTIR), as well as GC-ECD and GC-MS. γ irradiation of solid samples was conducted over a dose range of 0−83 kGy. On alumina in the presence of air, HCB was reductively dechlorinated to penta- and tetrachlorobenzene. No HCB reaction was observed on KBr, which served as a noncatalytic support to check the extent of direct radiolytic reaction. HCB conversion to dechlorinated products decreased as a function of increasing surface coverage on alumina, indicating the critical, catalytic role played by the support material. A reaction scheme is proposed.

Introduction

Metal oxides such as Al_2O_3 have relatively large band gaps (7 eV) and require high-energy excitations to produce charge separations.[1] There have been numerous studies of the use of ionizing radiation to produce excitations in metal oxide particles and subsequent charge transfer to molecules adsorbed at oxide surfaces.[2−5] An early study found that the γ-irradiation of *n*-pentane adsorbed onto various solids yielded product distributions that differed widely depending on the solid surface and were also very different from the results of bulk liquid radiolysis.[2] In general and in contrast to low-energy excitation, for systems of solids with coadsorbed molecules, high-energy radiation excites the solid structure-promoting chemistry in remote regions of the solid by producing ionizations of the solid and subsequent transfer of excitation energy to the adsorbate.[6] In this research the radiolytic transformation of hexachlorobenzene (HCB) on γ-Al_2O_3 is investigated in order to probe the potential role played by an oxide surface in the radiation-induced catalytic transformation of pollutants in environmental systems.

The principle of γ ray-induced charge separation and transfer processes in a metal oxide semiconductor is illustrated in Scheme 1.

Ultraband gap excitation of these oxide particles results in charge separation. These charge carriers in the conduction and valence bands recombine or migrate to the particle surface, where they become trapped, or participate in the interfacial oxidation and reduction of adsorbed species.[7]

In general, the radiolysis of solids with adsorbates produces ionic products and free radicals derived from these ions. Large radiation doses, >10 kGy, are generally thought to cause observable atom displacement in the crystal lattice, while at lower doses, <100 Gy, organic molecules adsorbed on the solids are degraded by transfer of the energy initially absorbed by the solid to the adsorbate.[2]

SCHEME 1. Possible Charge Separation and Heterogeneous Electron Transfer at a Metal Oxide Particle Using γ-irradiation.

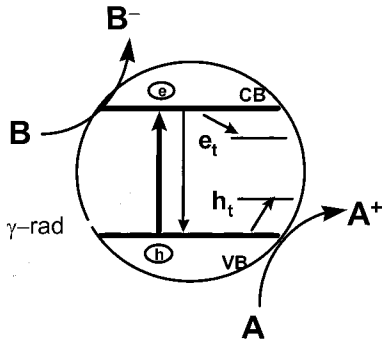

Irradiation of oxides may give rise to color centers that absorb in the UV and visible range. For instance, in SiO_2, UV-absorbing color centers are associated with trapped electrons, and visible color centers are associated with hole trapping on impurities. Visible color centers on Si/Al catalysts have been shown to catalyze chemical reactions.[6] The disappearance of trapped electrons and the UV color centers has also been shown to drive the conversion of isopropylbenzene to benzene.[8] On γ-Al_2O_3, many organic molecules bleach visible color centers.

Early study of the interaction of high-energy radiation with solid materials was important for the design of materials used in the nuclear industry. Current interest is also related to material durability issues and the design of materials for electronic

* To whom correspondence should be sent.
[†] Northwestern University (tel 847-467-4252; fax 847-491-4011; e-mail k-gray@nwu.edu).
[‡] University of Notre Dame (tel 219-631-5411; fax 219-631-8068; e-mail PKamat@nd.edu or http:/www.nd.edu/~pkamat).

10.1021/jp990211u CCC: $18.00
Published on Web 03/11/1999

applications.[9] In addition, activation of oxide nanoparticles by ionizing radiation may be a critical factor in the transformation or decay of pollutants present in complicated matrices such as high-level radioactive storage wastes or soils. Since the energy levels of the band edges are more energetic than those of lower energy band gap semiconductors, such as TiO_2, metal oxides excited by ionizing radiation may drive reactions having much higher redox potentials than photocatalysts stimulated by UV irradiation. For remediation applications, this is an attractive feature that is well adapted to the destruction of highly chlorinated pollutants, which are typically very refractory. Furthermore, radiation-induced reaction on metal oxides may have numerous possible applications in chemical production, reuse, or recovery where this feature, in combination with specific oxide surface chemistry, may provide reaction control and selectivity.

There is a general lack of fundamental knowledge about the radiolytic processes that control the fate of high level nuclear waste containing citrate, nitro- and halogenated organic compounds, EDTA-derived metal complexes, and metal oxide particles. The degradation of these organic compounds by γ radiation poses serious safety and pretreatment concerns because of the flammability and explosive hazards associated with the rates of production of hydrogen and low molecular weight, high vapor pressure organic compounds.[10] While the radiation chemistry of many hazardous organic compounds and metal complexes are well understood in homogeneous solvents, the kinetics and products may be quite different in heterogeneous media. For example, a recent study has shown that organic compounds adsorbed onto SnO_2 colloids react with aqueous electrons and hydroxyl radicals with rate constants that are an order of magnitude lower than those observed in water.[11] In contrast, radiolytic destruction of EDTA was enhanced by the presence of TiO_2.[10] Since these high-level tank wastes are heavily loaded with solid particles,[12] it is important to determine if the transfer of radiolytically generated charge carriers across the solid−liquid interface is significant under storage conditions. A recent study by Schatz et al. demonstrated that the irradiation of aqueous colloidal suspensions of SiO_2 resulted in an efficient production of hydrated electrons.[13] In summary, then, one cannot make reliable predictions of the course of radiolytic reactions under nonhomogeneous conditions using yields and rate data acquired in homogeneous systems.

Radiolysis has been reported to degrade completely a variety of pollutants in soil systems.[14−18] Recent work exploring the radiolytic transformation of HCB on a variety of soils has demonstrated that the rate and extent of reductive dechlorination are much greater in soils having high oxide or clay content.[19] One of the aims of this research, then, is to determine if the presence of an oxide can account for the accelerated HCB degradation observed in mineral soils. Since oxide and clay materials are large fractions of many soils, greater understanding of their role in the radiolytic degradation of pollutants may improve our ability to predict reactions in soils and other solid, environmental systems. Furthermore, this insight may provide us with strategies to control and target certain chemical transformations, allowing selective material modifications and improving our ability to design efficient radiation processes for environmental application. For example, the reductive dechlorination of HCB modifies its solubility and hence its bioavailability, as well as its overall biodegradability. Pretreatment of an excavated, contaminated soil by ionizing radiation may prove to be a highly effective means to enhance subsequent bioremediation.

The purpose of this research is to study and compare the radiation-induced chemical interactions of HCB adsorbed to alumina and KBr. The choice of HCB as a model pollutant was made based on the fact that it is a common soil contaminant associated with chemical manufacturing and use, and it is also a useful surrogate for a large class of chlorinated, hydrophobic, aromatic pollutants commonly encountered at environmental sites. Alumina was chosen as the model oxide in this study because of its general relevance to a wide range of applications, particularly those of environmental interest. For instance, various forms of aluminum oxides are found in natural soils over a wide range of concentrations.[20] In addition, alumina may also be a practical material with which to amend contaminated materials to achieve a desired chemical conversion. Furthermore, aluminum oxides and oxyhydroxides are significant components of tank wastes and in some cases are present at concentrations greater than any other oxide solid.[21]

To determine alumina's reactivity under γ irradiation, experiments were conducted in the solid state and reaction products were monitored by diffuse reflectance UV and FTIR spectroscopy. Products were also identified and quantified by gas chromatography with electron capture detection (GC-ECD) and gas chromatography−mass spectroscopy (GC-MS). In addition, the effect of surface concentration on reaction rates was also explored.

Experimental Section

Sample Preparation. Alumina samples were obtained from Degussa Corporation (Akron, OH) and HCB from Aldrich (Milwaukee, WI). These chemicals were of the highest purity and were used as received without further purification. A single, monolayer coverage of HCB was defined as a single layer of HCB, one molecule thick, covering the total surface of alumina and was produced using approximately 46.5 mg of HCB per gram of alumina (0.16 mmol/g Al_2O_3). The monolayer mass of HCB required per gram of alumina was calculated based on a particle surface area of 100 m^2/g and an average diameter equal to 20 nm for alumina and an assumed molecular area for HCB of 10 $Å^2$. To test for catalytic activity, samples were prepared with 0.5, 1.0, and 2.0 monolayer surface coverage. Desired amounts of alumina and HCB were weighed out, placed in a flask, and mixed thoroughly with 250 mL of 1:1 acetone/hexane solution until HCB was thoroughly dissolved. Using rotary evaporation under vacuum, the volume of the sample was reduced to approximately 30 mL. It was then transferred to a 50 mL vial and allowed to dry in an oven at 50 °C overnight.

Samples of HCB adsorbed to a noncatalytic support, KBr, were also prepared by this method. KBr was oven dried overnight at 104 °C to remove adsorbed moisture and then thoroughly ground prior to HCB application. The KBr particles prepared in this way, however, varied in size and surface area. Thus, the mass of HCB adsorbed to KBr was set arbitrarily at 23 mg HCB/g KBr, half that used in the alumina experiments. Although the mass of HCB required for monolayer coverage could not be determined accurately, it is estimated that under these conditions surface coverage was greater than monolayer. The sole purpose of KBr experiments was to evaluate the extent of direct radiolytic reaction of HCB on a noncatalytic support. Although multilayer coverage influences surface-induced catalytic reactions, it has no effect on direct radiolytic interactions.

UV-Diffuse Reflectance Measurements (UV-DR). The diffuse reflectance absorption spectra of HCB adsorbed to Al_2O_3 and KBr were recorded with a Shimadzu UV-3101PC, UV−vis spectrophotometer. Reflectivity of solid-state samples was

monitored using a diffuse reflectance attachment in an open atmosphere at room temperature. A thin layer of irradiated powder (~0.05 g) was prepared between two quartz slides and inserted into the spectrophotometer for measurement. Spectra were recorded at a slow scan rate in 0.2 nm increments over a range of 200−400 nm. This analytical window was chosen due to the general noise of alumina in the 400−800 nm region. Clean alumina and KBr, as well as nonirradiated HCB/Al_2O_3 and HCB/KBr, served as controls. Results are expressed in the units of Kubelka−Munk, $(1 - R)^2/2R^2$, for semiquantification of HCB decay.[22] Using this relationship, reflectance data may be transformed into units which directly correlate surface concentration to absorbance.

Fourier Transform Infrared (FT-IR) Measurements. All FTIR experiments were performed using a Bio-Rad FTS 175, FTIR spectrometer with a diffuse reflectance accessory. Samples were placed within micro sampling cups for analysis inside the instruments' nitrogen-purged chamber to prevent interference by CO_2. The diffuse reflectance spectra of all samples were measured in the region 400−4000 cm^{-1} at a resolution of 8 cm^{-1}. In most cases no enhancement in spectral features was observed when the resolution was increased from 8 to 4 cm^{-1}. Hence, the spectra were all obtained at 8 cm^{-1} resolution. In the case of alumina samples, a much smaller analytical window of 1000−2000 cm^{-1} was analyzed due to noise from alumina outside this energy range.

***γ* Radiolysis.** Radiolysis of all samples was performed using a Shepard-109, ^{60}Co source. ^{60}Co is an emitter of high energy, 1.25 MeV, photons (γ-rays). The Shepard-109 is a concentric well type source with a dose rate of approximately 69 Gy/min. This dose rate was calculated in our laboratory using Fricke dosimetry.

FTIR samples were irradiated in diffuse reflectance sampling cups to prevent variation in the location of samples with respect to the FTIR infrared beam. Samples were irradiated under an open atmosphere, and the dose was applied in an additive fashion. Initially, the spectrum of an individual sample was recorded prior to radiolysis. After a given time period of irradiation, the sample was removed from the γ cell and another spectrum was recorded. This process was repeated again and again for all samples until a cumulative dose of 82.8 kGy was achieved.

Individual sample vials (7 mL) containing approximately 0.2 g of solid sample were irradiated to produce samples for UV-DR and GC measurements. These samples were irradiated under a headspace of air.

Extraction and Analysis. All samples were analyzed by conventional GC techniques in addition to FTIR and UV-DR. Compounds bound to alumina were extracted in sample sizes of approximately 0.10 g with a 1:1(v/v) solution of acetone and hexane. An internal standard 1,3,5-tribromobenzene at a concentration of 4 mg/L was added to adjust responses for extraction efficiency and changes in volume. 1,3,5-Tribromobenzene was used as an internal standard because of its structural similarity to HCB and high response in electron capture detectors (ECD). Samples were then sonicated for 5 min to enhance desorption of HCB from the oxide surface. Resulting suspensions were centrifuged for 3 min at 890*g* to remove the majority of oxide particles from suspension, thus producing a relatively clean sample for injection into the GC interface. In this research, ECD detection was first used to identify tentatively and quantify compounds, with subsequent verification using GC-MS.

A method for the detection and quantification of HCB and reduced forms of HCB using GC-ECD was established in previous research.[19] Extracted samples were analyzed using a Hewlett-Packard series 4890 GC with ECD detection. A Restek RTX-5 nonpolar column was used with helium as a carrier gas and an argon/methane (P-5) gas mixture for ECD makeup.

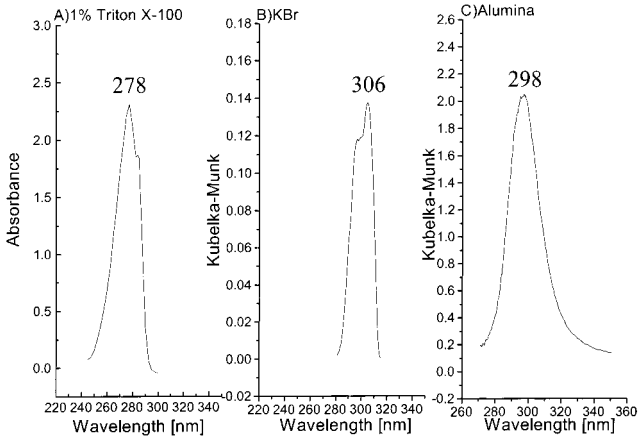

Figure 1. UV absorption spectra of HCB (a) in 1% Triton X-100 Surfactant (50 μM), (b) adsorbed onto KBr, (c) adsorbed onto alumina (1.0 monolayer).

Verification of products was achieved through the use of a Hewlett-Packard 6890 GC-MS. Mass spectra were compared to NIST databases for tentative identification and compared to standards for final confirmation. For GC-MS work, a J&W Scientific DB-5 column was used, and the oven programming was identical to that used for GC-ECD runs.

Results

Sorbed and Aqueous Phase HCB. In Figure 1, the UV absorption spectra of HCB in 1% Triton X-100 surfactant solution, in a single monolayer on KBr, and in a single monolayer on Al_2O_3 are compared. In all three cases, the HCB spectra show a single peak which is representative of the $\pi \rightarrow \pi^*$ transition in the aromatic C═C double bond.[23] The surfactant solution and KBr spectra both display the presence of a shoulder peak. In the case of KBr samples, this shoulder peak is attributed to the general noise of the KBr sample. However, the shoulder peak in the spectrum of HCB in Triton X-100 is the result of the weaker E_2 band absorption of the aromatic ring.[23] The absorption maximum of HCB in the aqueous phase appears at a wavelength of 278 nm. In contrast, the absorption maximum occurs at 306 nm when HCB is adsorbed to KBr and at 298 nm when adsorbed to Al_2O_3. In general, Figure 1 illustrates the occurrence of a large red shift in the absorption spectra of HCB when adsorbed to solid surfaces. This shift is attributed to a limited torsional mobility of the HCB molecule.[24]

In Figure 2 the FTIR spectra of HCB neat (Figure 2a) and HCB adsorbed to alumina (Figure 2b − 1.0 monolayer coverage) are compared. The two large bands at 1336 and 1296 cm^{-1} in the neat spectrum, as well as the bands at 1345 and 1296 cm^{-1} in the HCB/Al_2O_3 spectrum, are attributed to the stretching of aromatic C═C bonds.[25] A direct result of HCB adsorption to the surface of alumina is the suppression of HCB molecular bending and torsion, which corresponds to a change in the relative intensity of certain peaks (1336 and 1296 cm^{-1}), a slight lateral shift of one of the aromatic bands (1336 cm^{-1} neat to 1345 cm^{-1} adsorbed), and the overall elimination of others (1919, 1216, and 1108 cm^{-1}) (Figure 2a). The spectrum of neat HCB shows a large region (1600−1375 cm^{-1}) of overtone bands from C−Cl bending bands.[26] The HCB/Al_2O_3 spectrum contains a region of peaks (1580−1500 cm^{-1}) that is attributed to

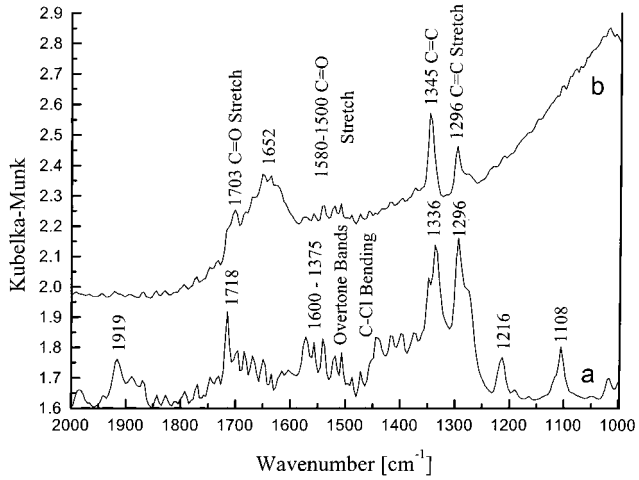

Figure 2. FTIR absorption spectra of (a) neat HCB, (b) 1.0-monolayer coverage of HCB on alumina.

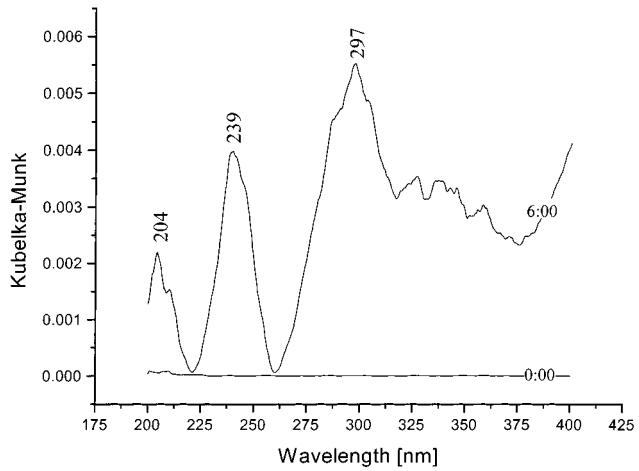

Figure 3. Diffuse reflectance absorption measurement of clean, nonirradiated and irradiated (6 h) alumina.

commonly adsorbed bicarbonate ions on the surface of alumina particles.[27] Such bands are the result of asymmetric stretching modes of the CO_2^{3-} ion.[28−30] However, remnants of the C−Cl overtone bands similar to those found in the neat HCB spectrum cannot be completely ruled out. The presence of a large, broad peak at 1652 cm^{-1} in the HCB/Al_2O_3 spectrum is found. This peak may be due to impurities on the oxide surface and/or moisture adsorption. Finally, the peak at 1703 cm^{-1} in the HCB/Al_2O_3 spectrum is associated with residual acetone adsorbed to the surface of alumina, an artifact of sample preparation. A sample of alumina, which had been mixed with acetone and hexane, showed the presence of this peak; clean alumina samples did not.

^{60}Co-Irradiated Alumina. Figure 3 illustrates the changes occurring in the UV-DR spectrum of uncoated alumina upon radiolysis. A clean sample of alumina shows a relatively flat line with no major absorption characteristics. As alumina is subjected to γ-radiation for 6 h, new absorption features appear such as those at 204, 239, and 297 nm. It is important to note, however, that the magnitude of absorbance of the irradiated alumina blank was much lower than what was witnessed in samples of HCB-coated alumina.

Past research has shown that γ-irradiation of γ-Al_2O_3 or silica−alumina produces trapped species.[5] The visible coloration observed in these irradiated samples is attributed to hole trapping that can be bleached upon exposure to molecules such as H_2, but not O_2.[6] UV-absorbing color centers may also correspond

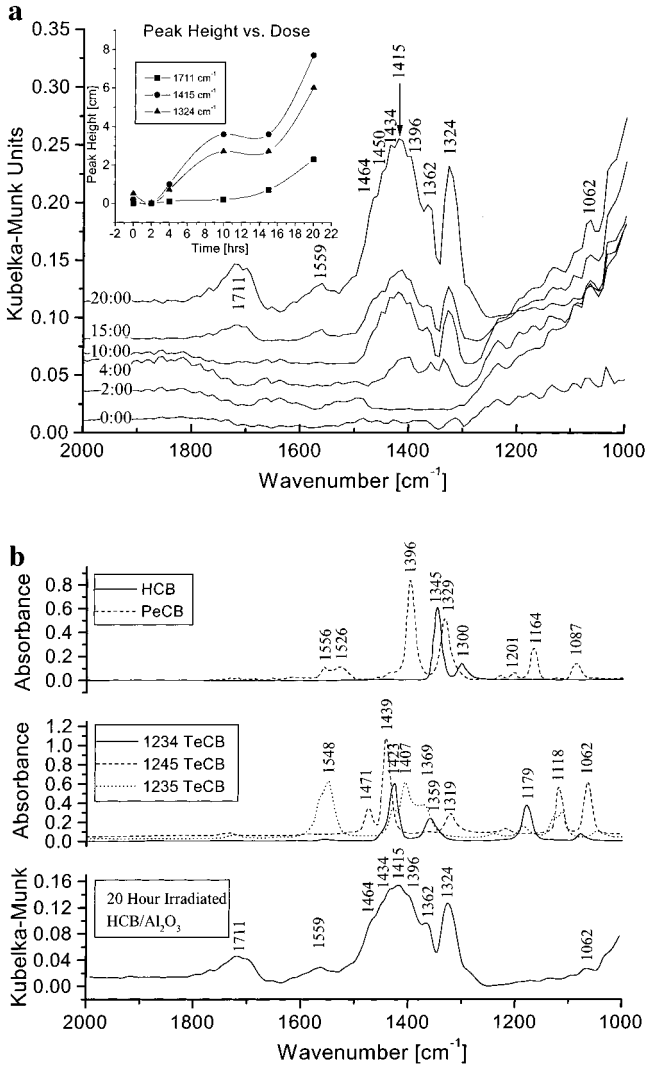

Figure 4. (a) FTIR spectra of HCB adsorbed onto alumina (1.0-monolayer) following of 20 h γ-irradiation period. (b) Comparison of reference FTIR spectra for HCB and reduced forms of HCB to the 20 h spectrum of 1.0-monolayer HCB adsorbed to alumina.

to trapped electrons. Shafeev found a very prominent absorption band between 280 and 400 nm following the irradiation of alumina with a 308 nm laser.[32] Agullo-Lopez and co-workers suggested that this damage was due to F2 color centers.[33] An F2 center is the trapping of two electrons in two adjacent anion vacancies within the crystal lattice.

The characteristics observed in Figure 3 are due to UV-absorbing color center formation or some other form of crystal damage. In our experiments, samples were not annealed following irradiation, a treatment that removes color centers. Given the measurable, albeit small, effect of irradiation on the UV absorption spectra, the formation of F2 centers has the potential to confound UV-DR measurements slightly. Nevertheless, Figure 3 supports the claim that alumina absorbs radiation and is capable of trapping charge carriers. FTIR analysis of irradiated, clean alumina samples, however, did not show spectral evidence of color centers.

FTIR Monitoring of ^{60}Co-Irradiated HCB/Al_2O_3. FTIR measurement of irradiated, single monolayer coverage of HCB on alumina is presented in Figure 4A. The spectra corresponding to 0−20 h of HCB/Al_2O_3 irradiation illustrate many changes in the samples. Within 10 h, a broad peak at 1415 cm^{-1}, as well as sharp and defined peak at 1324 cm^{-1}, appeared. At the end of a 20-h irradiation period, new peaks at 1711, 1559, and 1062

cm^{-1} were observed. Upon closer inspection of the 20-h spectrum, the large peak at 1415 cm^{-1} appears to be the result of the constructive interference of several peaks. Shoulder peaks are evident at 1464, 1450, 1434, 1396, and 1362 cm^{-1}. The insert of Figure 4A shows the growth rate of the three largest peaks including the conglomerate at 1415 cm^{-1} over a 20-h period. The FTIR peaks at 1415 and 1324 cm^{-1} grow in a similar fashion, while the growth of peak 1711 cm^{-1} increases steadily with time after an initial lag period.

The region at ~3600 cm^{-1} (not shown) was scanned for the presence of a large stretch band indicative of an −OH bond. Such a band would reflect the hydroxylation of HCB and the formation of a chlorophenol.[26] Since a band in this region was not found, oxidation of HCB was concluded not to have occurred under the conditions of these experiments.

Figure 4B compares reference (gas phase) infrared spectra[25] for HCB, pentachlorobenzene (PeCB), all three isomers of tetrachlorobenzene (TeCB) and the 20-h spectrum of HCB/Al_2O_3. The dechlorination of HCB leads to changes in molecular symmetry that, in turn, transform the HCB infrared spectrum as shown. Chlorine loss results in more secondary aromatic peaks (1200−1000 cm^{-1}). Comparison of the 20-h spectrum to the HCB and PeCB spectra shows little agreement. However, further comparison between the 20-h spectrum and the TeCB spectra demonstrates that the 20-h spectrum is explained well by the TeCB reference spectra. It is worth noting that a feature common to the FTIR spectra of all irradiated samples is the breadth of the peaks, and in this case, broadening is due to surface adsorption. Since most FTIR peaks arise from the stretching of C═C bonds, the FTIR band broadening may be associated with the adsorption of the aromatic ring to Lewis acid functional groups on the surface of alumina.[34−36]

Bearing in mind that peaks tend to broaden, we found that all of the peaks in the 20-h spectrum (including the conglomerate at 1415 cm^{-1}) are explained by the contribution of TeCB isomers in the region from 1600−1250 cm^{-1}. Additive contributions, in addition to band broadening, give rise to the shoulder peaks at 1464, 1434, 1396, and 1362 cm^{-1}, as well as the secondary peak at 1062 cm^{-1}. Though the contribution of PeCB to the 20-h spectrum is unclear, it appears that the overall contribution from HCB is small due to the presence of a valley in the 20-h spectrum between the shoulder peak at 1362 cm^{-1} and the peak at 1324 cm^{-1}. If HCB significantly contributed to the 20-h spectrum, we would expect to observe the presence of a C═C stretch band at 1345 cm^{-1} in the HCB spectrum.

The peak at 1711 cm^{-1} in the 20-h spectrum is explained by the contribution of TeCB bands (C−Cl overtone bands) and/or surface bound −COOH groups. The 1650−1750 cm^{-1} region is typical of the C═O stretch found in carboxylic −COOH groups.[26] In addition, traces of acetone, the solvent used in sample preparation, may also contribute to the band at 1711 cm^{-1}. Other secondary bands in the region of 1200−1000 cm^{-1} of the TeCB spectra appear to have little contribution in the 20-h spectrum of HCB/Al_2O_3. As shown, these peaks have been severely suppressed with only the peak at 1062 cm^{-1} discernible. This is consistent with surface adsorption; recall that, when comparing the spectrum of neat HCB and HCB adsorbed to alumina, a large degree of peak suppression was observed in this same region (Figure 2).

The relative distribution of each transformation product was estimated by comparing the 20-h spectrum to the reference spectra presented in Figure 4b. All spectra were normalized before evaluation. HCB, PeCB, and the three isomeric forms of TeCB were entered into a Matlab program as peaks, defined by their area, width, and location. These coordinates were then fit to a series of overlapping Lozentzian line shapes so that artificial band widening was possible.[37] These "new" broadened spectra were then compared to the 20-h spectra using a nonnegative least-squares fitting routine. This routine finds the optimal linear combination of the reference spectra that would yield the 20-h HCB/Al_2O_3 spectrum. Table 1 lists the estimated percent contribution of TeCB species to the 20-h HCB/Al_2O_3 spectrum as predicted by this algorithm.

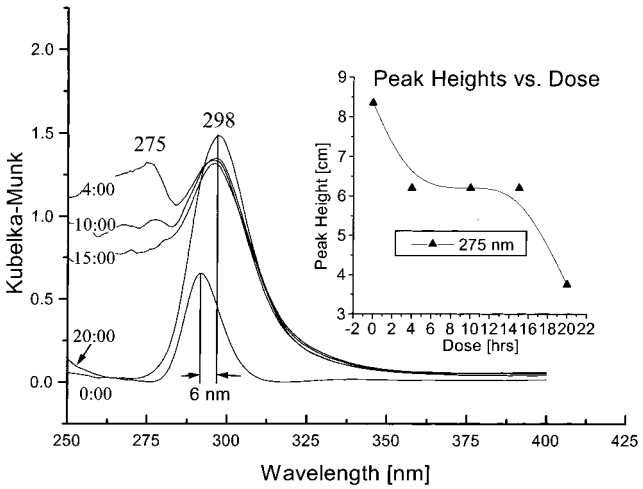

Figure 5. Diffuse reflectance absorption spectra of HCB adsorbed onto alumina (0.5-monolayer). Spectra were recorded at different γ-irradiation intervals (hr).

TABLE 1: Byproduct Proportions

compound	% contribution
1,2,3,4-TeCB (ortho)	14
1,2,3,5-TeCB (meta)	11
1,2,4,5-TeCB (para)	75

The relative distribution of the TeCB isomers is consistent with what would be expected; degradation from PeCB to TeCB proceeds primarily through the removal of the para position chlorine atom.

UV-DR Measurements of ^{60}Co-Irradiated Alumina/HCB. Figure 5 shows the transformation of 0.5-monolayer coverage HCB/Al_2O_3 under radiolysis as measured by UV-DR. The nonirradiated HCB/Al_2O_3 sample exhibits a large $\pi \rightarrow \pi^*$ transition absorbance at 298 nm as shown by the zero hour control. Irradiation with high-energy photons induces rapid transformation and the formation of an intermediate peak at 275 nm. As mentioned previously, alumina was found to trap electrons near this region as shown in Figure 3, and therefore the intermediate at 275 nm is attributed to the presence of trapped charges. The insert in Figure 5 shows the growth and decay of peak 275 nm with time. Since the time between irradiation and measurement varied between samples, there is a corresponding variation in trapped species concentration due to decay. The peak at 275 nm is an indicator of trapped electrons, the height of which decreases with time.

Another noticeable effect of radiolysis is the 6 nm blue shift occurring in the UV spectrum from 0 to 20 h. As molecules become more polar there is, in most cases, a blue shift in the UV spectrum.[38] Electrophilic groups such as chlorine atoms lead to a shift in aromatic absorption. More specifically, it is shown that the addition or subtraction of a chlorine atom from an aromatic ring will shift the absorption of the aromatic molecule by 6 nm.[23] We therefore conclude that Figure 5 is evidence of HCB transformation to PeCB. It is interesting to note that, while FTIR spectra show clear formation of TeCB, the existence of a

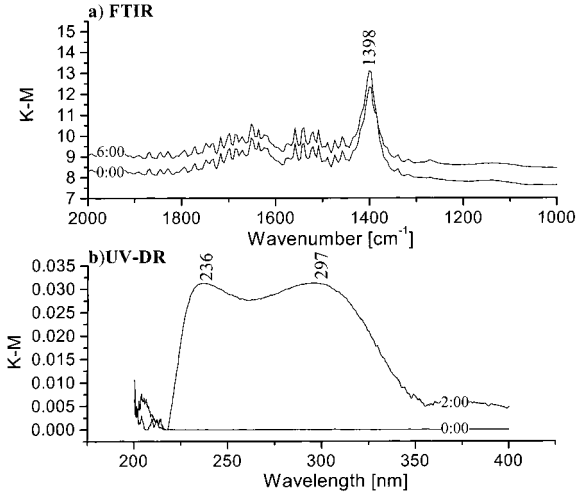

Figure 6. Diffuse reflectance FTIR and absorption measurement of (a) clean, nonirradiated and (b) γ-irradiated (2 h) KBr.

blue-shift greater than 6 nm is not detected. This is attributed to the low extinction coefficient of TeCB isomers which translates into poor absorbance at low concentrations on the surface of alumina.[38] As a result, TeCB detection was not possible by UV-DR.

Irradiation of KBr Blank with ^{60}Co. Figure 6 displays the changes that occur to KBr blanks under radiolysis. Pure KBr samples lead to a spectrum of high absorbance. Little change is observed in the FTIR spectra (Figure 6a) over a 6-h dose period. In contrast, Figure 6b shows two very large, overlapping peaks (236 and 297 nm) in the UV-DR spectrum of a 2 h irradiated KBr sample. These changes in UV absorption are explained by the production of color centers in the KBr crystal lattice. Many forms of radiation, including γ-rays, have been shown to produce F (trapped electrons) and other color centers in halide crystals.[39,40] Experiments with KBr showed blue coloration in the presence of γ-rays, indicative of trapped electrons. This color disappeared as samples were allowed to lie idle at room temperature (298 K). However, not all trapped electrons and holes may have had sufficient time to decay at room temperature (as was the case with alumina samples), because the time between irradiation and measurement varied slightly. It has been shown that strong and broad absorbance in the range of 220−350 nm typically corresponds to V-type color centers caused by trapped holes.[41] A V center is defined as a halogen atom which spans two adjacent anion sites to give an overall positive charge. The change in absorbance may also be due to surface defects produced via radiation of the crystal lattice of KBr.[42] Clearly the measurements of HCB adsorbed to KBr using UV-DR are affected by the presence of color centers and crystal lattice damage. It is important to note, however, that even though the units of absorbance (UV) are low for the 2 h KBr sample in Figure 6, this sample underwent some color center decay prior to measurement. It can also be seen from Figure 7b that the difference between the 0 and 2 h maximum absorption values is about 0.05, a value comparable to, although greater than, the absorption maximum in Figure 6.

Irradiation of HCB Adsorbed KBr with ^{60}Co. Experiments with HCB adsorbed to KBr were performed to determine the extent of direct HCB degradation by γ-rays. Since KBr is an ionic crystal, it does not contain unoccupied electronic levels; therefore, charge separation is not possible.[43] KBr, then, is expected to be noncatalytic and inert toward surface-promoted electron-transfer processes. Figure 7a shows the FTIR spectra of HCB/KBr irradiated samples. The high (23 mg HCB/g KBr)

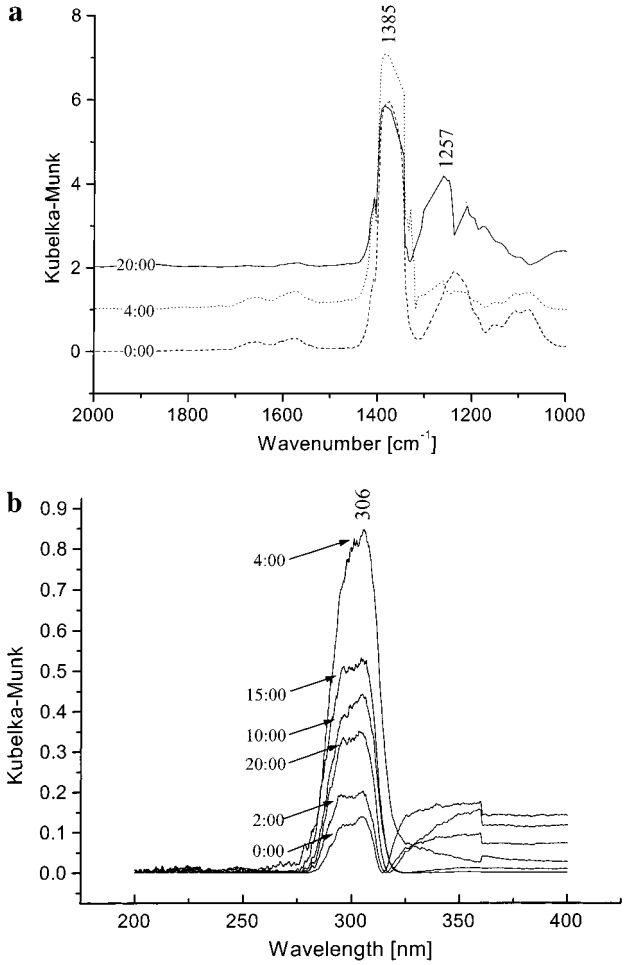

Figure 7. (a) FTIR spectra of HCB adsorbed onto KBr and (b) diffuse reflectance absorption measurement of HCB adsorbed onto KBr, recorded following γ-irradiation.

concentration of HCB on the surface of KBr leads to high adsorption units as well as producing very broad peaks. The two peaks at 1385 and 1257 cm^{-1} are aromatic, C═C stretching bands which are broad and shifted in comparison to those (1345 and 1296 cm^{-1}) in the spectrum of HCB adsorbed to alumina (Figure 2b). Although there are some nominal changes to the spectra in the 1600−1200 cm^{-1} region, there are no signs of PeCB and TeCB formation as was found in the 20 h dose of HCB/Al_2O_3 (Figure 4b). This observation is one piece of evidence demonstrating that HCB was not degraded (directly) by γ radiation.

Analysis of irradiated HCB/KBr samples by UV-DR exhibited a large, dominant ring absorption peak at 306 nm as shown in Figure 7b. Variation in absorbance is attributed to the production and varying decay of V or H (interstitial halogen atom) centers in blank KBr as shown by experiments with KBr blanks (Figure 6). This interference leads to the variation in the height of the aromatic peak as shown. The region from approximately 320 to 375 nm showed small baseline fluctuations, an effect seen only in KBr samples and believed to be a result of matrix effects. No changes in the baseline between 200 and 275 nm were witnessed nor was the blue-shift found in HCB/Al_2O_3 samples (Figure 5) observed. The absence of a blue shift in the UV-DR spectra further points to the lack of HCB conversion by direct radiolysis.

Comparison of Samples with Different HCB Surface Coverage. HCB was adsorbed to alumina in concentrations that resulted in 0.5-, 1.0-, and 2.0-monolayer samples. If alumina

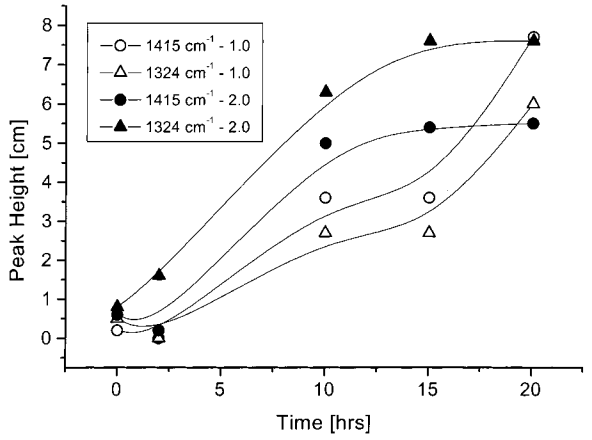

Figure 8. Comparison of peak heights in FTIR spectra as a function of HCB surface coverage (1.0- and 2.0-monolayer) of γ-irradiated Al_2O_3 samples.

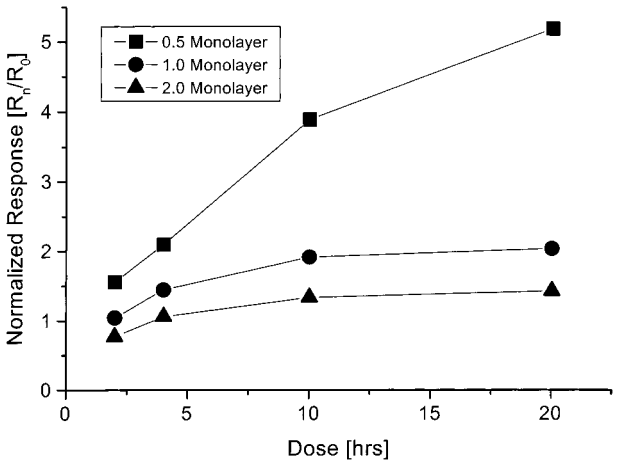

Figure 9. Formation of pentachlorobenzene over time as a function of HCB surface coverage following γ-irradiation.

catalysis were induced by radiation, then one would expect catalytic activity to decrease as a function of increasing surface coverage. As surface coverage increases, we would expect surface sites to become limiting and ultimately saturated. This phenomenon demonstrates that HCB reaction requires direct interaction with the alumina surface.[44] Figure 8 compares the heights of the two prominent peaks, 1324 and 1415 cm^{-1}, found in the FTIR spectra of irradiated 1.0- and 2.0-monolayer HCB/Al_2O_3 samples. Recall that earlier we determined that these two peaks correspond to PeCB and TeCB formation, respectively (Figure 4b). At lower HCB coverage, the growth of these two peaks is positive and upward. In contrast, greater HCB coverage results in asymptotic peak growth that exhibits saturation-type kinetics.

Byproduct Analysis. Extraction of adsorbed material on alumina samples allowed for the analysis of HCB byproducts by conventional GC techniques. GC-ECD analysis detected the presence of pentachlorobenzene (PeCB) and tetrachlorobenzene (TeCB). Verification as to the form (reduced or oxidized) of degraded HCB was achieved through GC-MS. GC-MS detected the presence of PeCB but not TeCB. Given the high sensitivity of ECD detectors toward halogenated aromatics, GC-ECD was therefore used for all quantification purposes. Only one TeCB isomer (1,2,3,4-TeCB) was quantifiable due to the coelution of the remaining 1,2,3,5-TeCB and 1,2,4,5-TeCB isomer forms of TeCB, and its concentration was 34.12 ppm. Coelution of the meta and para isomers has been found elsewhere in GC work.[45] However, on the basis of FTIR results, if the concentration of 1,2,4,5-TeCB is assumed to be much greater than the concentration of 1,2,3,5-TeCB, the concentration of 1,2,4,5-TeCB is estimated to be 107 ppm from GC-ECD results. This is three times the concentration found for the 1,2,3,4-TeCB isomer. The GC-ECD results, then, reflect the same trend in relative concentrations of the TeCB isomers as that determined by FTIR (Table 1). The quantification of isomer concentrations by GC-ECD and FTIR are in similar ranges, but differ in absolute concentrations given the accuracy of quantifying the FTIR spectra.

Figure 9 is a plot of normalized responses for PeCB from GC-ECD analysis. Comparison of PeCB responses for all three surface concentrations leads to the conclusion that PeCB growth was the greatest in samples with a surface coverage of 0.5-monolayer. Growth for 1.0- and 2.0-monolayer coverage was similar in shape and illustrates reduced PeCB production with increasing surface coverage. Again, as the surface coverage of HCB increases, direct surface interactions between the HCB molecule and reactive intermediates are blocked, leading to a decrease in the catalytic process of transformation. Research with compounds adsorbed to TiO_2 have shown similar dependence of catalytic reaction on surface coverage.[46,47] More importantly, the extraction of KBr samples yielded little to no PeCB, demonstrating that direct radiolytic reaction did not occur. The charge-transfer processes mediated by the alumina surface are required for the conversion of HCB to PeCB and TeCB.

TABLE 2: Measured Species Concentrations and Calculated *G*-Values

compound	Concn [ppm]	std dev [ppm]	*G* [mol/100 eV]
PeCB	546	45	2.5×10^{-5}
1,2,3,4-TeCB	34	5	1.8×10^{-6}
1,2,4,5-TeCB	107	9	5.8×10^{-6}
$TeCB_{total}$	141	10	7.6×10^{-6}

Since quantification was possible for PeCB and 1,2,3,4-TeCB and the concentration of 1,2,4,5-TeCB could be estimated based on FTIR results, *G*-values were calculated to determine radiolytic yields. *G* is defined as the number of molecules produced or lost per 100 eV of energy absorbed.[48] It is important to note that since we are working in the solid-state, the exact absorbed dose is not precisely known. In this case, *G*-values were calculated using the applied dose. *G*-values and the concentration (mg analyte/kg Al_2O_3) of byproducts in a 20-h (82.8 kGy), 1.0-monolayer HCB/Al_2O_3 sample are presented in Table 2.

Low *G*-values are common for solid-state radiolysis in which degradation proceeds by direct or direct-like effects. Direct effects literally involve the direct hit of the target molecule by a photon resulting in a radical cation−electron pair or an excited target molecule. Direct-like effects involve interactions between a target molecule and secondary, thermalized electrons, which result from the interaction of high-energy photons with the solid matrix. Past research by Hilarides et al. found *G*-values associated with direct-like effects in the range of $1.4-9.6 \times 10^{-6}$ for concentrations of 100 ng/g of 2,3,7,8-tetrachlorobenzo-*p*-dioxin (TCDD) in various matrixes.[16] The *G*-values listed in Table 2 clearly point to radiolytic reaction via direct-like effects, though they are somewhat greater in value, suggesting enhanced degradation over ordinary direct-like effect mechanisms. This is another indication of catalysis.

Discussion

Steady state, γ-irradiation of HCB-coated alumina at a dose of 82.8 kGy resulted in the catalytic conversion of HCB on the alumina surface. A suite of analytical methods including UV-

DR, FTIR, and conventional GC and GC-MS techniques were used to probe the surface reactions and illustrate that HCB adsorbed onto an oxide support is reductively dechlorinated. Although complete dechlorination was not achieved over the radiation dose tested, complete pollutant destruction has been demonstrated at higher doses in previous research.[19] The absence of HCB reaction on KBr powder, a noncatalytic support, demonstrates that direct interaction with γ-irradiation alone fails to produce HCB conversion.

FTIR results showed the appearance of many new bands that are attributed to TeCB production. In addition, UV-DR studies showed a 6 nm shift in HCB spectra, which is also in agreement with the dechlorination of HCB. UV-DR results of HCB adsorbed to KBr showed some changes in the UV spectra including the vertical variation in aromatic absorption. This phenomenon, however, is attributed to the formation of color centers that affect the absorption characteristics of the samples. Although color centers were found to occur in HCB/Al_2O_3 samples as well, the magnitude of their absorbance was small relative to that of HCB and its reaction byproducts.

Further analysis of samples using GC-MS and GC-ECD allowed for the identification and quantification of PeCB and TeCB present on the surface of alumina. The rate and extent of PeCB formation was directly dependent and inversely proportional to HCB surface coverage. Higher HCB surface coverage on alumina caused the blocking of active surface sites and the reactive intermediates necessary for HCB transformation. Previous observations have shown that radiation induced charges move about 50 Å from their initial site of creation to the site of the adsorbate, implying that intimate contact between HCB and the alumina surface is required for transformation.[6] In addition, calculated yields, or *G*-values, fall in the range expected for direct-like effects or energy transfer from the solid to an adsorbed substrate. In comparison to literature values for radiolytic transformation of pollutants on solid environmental matrixes,[16] the *G*-values calculated for these experiments are approximately 1 order of magnitude greater which may reflect the enhancing effect of oxide catalysis.

As shown in the Scheme 1, absorption of γ rays by Al_2O_3 nanoparticles results in charge separation, similar to that observed for semiconductor particles with UV or visible irradiation. Earlier radiolytic studies with silica and zeolites have shown that ionization events in these solids are similar to those in nonpolar media.[6,9,49] γ rays are energetic enough to create electron−hole pairs in oxide particles, most of which recombine within first few picoseconds to produce triplet excitons. A fraction of these charge carriers are also trapped at defect sites. Research with silica has shown that both triplet excitons and trapped electrons can react with surface-bound OH groups to generate H-atoms.[9,50] Holes, on the other hand, react with H-atoms and surface-bound hydroxyl defects in the oxide layer to form surface-bound protons and hydroxyl radicals, respectively. Surface-adsorbed aromatic species may interact with the H-atoms to undergo H-addition and, in the case of HCB, dechlorination. In experiments where silica was pretreated at higher temperature to drive off surface-bound water and hydroxide, subsequent irradiation produced ionized products of the adsorbed aromatic compounds due to decreased H-atom production. Radiolytic homolysis of the hydroxyl group O−H bond and dissociative electron attachment to silanol groups have been proposed to account for H-atom production in irradiated silica.[6,9]

Since, in this work, radiolysis was carried out in air without pretreatment, one would expect H-atom formation in irradiated

SCHEME 2. Dechlorination Mechanism.

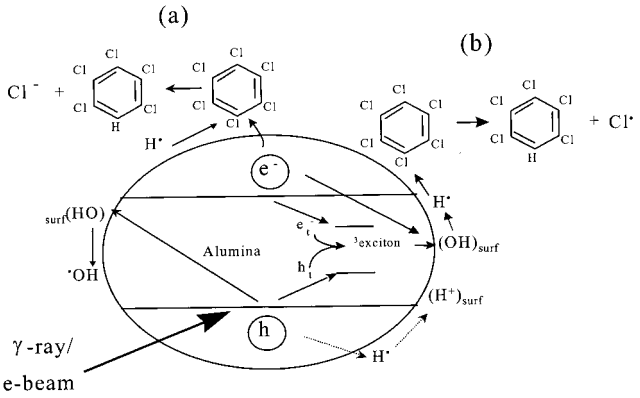

Al_2O_3 samples (reactions 1 and 2).

$$-\mathrm{M}-\mathrm{OH} + {}^3\mathrm{exciton} \rightarrow -\mathrm{MO}^{\bullet} + \mathrm{H}^{\bullet} \quad (1)$$

$$-\mathrm{M}-\mathrm{OH} + \mathrm{e}^{-} \rightarrow -\mathrm{MO}^{-} + \mathrm{H}^{\bullet} \quad (2)$$

−M−OH refers to OH groups bound to a metal oxide surface. While the fate of holes is not exactly known, one would expect them to generate •OH radicals by reacting with surface hydroxyl groups or to be scavenged by H-atoms to produce lattice-bound protons.

$$-\mathrm{M}-\mathrm{OH} + \mathrm{h} \rightarrow -\mathrm{M}^{+} + {}^{\bullet}\mathrm{OH} \quad (3)$$

$$\mathrm{H}^{\bullet} + \mathrm{h} \rightarrow \mathrm{H}^{+} \quad (4)$$

Holes also become trapped quite efficiently in alumina samples to form visible coloration. Direct interaction of HCB with electrons and/or reaction with H atoms is proposed to produce dechlorination, as shown to occur with the transformation of HCB to pentachlorobenzene in Scheme 2, reactions a and b.

Choi and Hoffmann found photoreduction of carbon tetrachloride in which the transfer of conduction band electrons formed trichloromethyl radicals and chloride.[51] Similarly, the reaction of HCB with conduction band electrons to yield chloride and pentachlorobenzyl radicals is possible prior to protonation (Scheme 2, a). Pulse radiolysis studies by Terzian et al. showed that reaction between aqueous electrons and pentabromophenol resulted in dehalogenation to produce a hydroxyphenyl radical.[52] On the basis of previous work, then, it is postulated that the role of trapped electrons and holes, as well as conduction band electrons, is central to the degradation of surface adsorbed HCB on alumina. The absence of a hydrogen source (surface hydroxyl groups), as well as the inability for charge separation to occur in KBr, explains why HCB degradation did not proceed when adsorbed to KBr.

Given the number of components and phases, many of which are unknown, and the complexity of interactions in the heterogeneous mixtures comprising environmental systems, it is very challenging to obtain a fundamental understanding of those radiolytic reactions which determine the fate of pollutants. Since metal oxides are major components of many environmental systems, it is important to elucidate their role in the radiolytic degradation of organic contaminants. In the case of high-level radioactive tank wastes, the build-up of volatile gases from the radiolytic degradation of organic compounds poses a significant safety hazard. Since it is imperative that accurate models are formulated to predict the course of these reactions,

it is essential to determine how metal oxides influence the chemical pathways and reaction kinetics of organic radiolysis.

Another environmental application of this work is in the area of soil remediation. Previous work has shown that rapid and complete dechlorination of HCB was achieved in soils having relatively low organic content and high levels of clays or silicates.[20] Although contaminant partitioning to the soil organic matrix interferes with radiolytic destruction somewhat, this effect can be reduced through the addition of higher levels of surfactant. The presence of clays and oxides in a system such as this may enhance radiolytic destruction of adsorbed pollutants. This observation, coupled with the research findings presented herein, indicates that it may be possible to enhance or control radiolytic reactions in environmental systems by the addition of metal oxides or natural zeolites, such as clays.

Conclusions

The catalytic degradation of HCB adsorbed to alumina colloids was demonstrated in the presence of γ-radiation. Degradation was shown to be dependent upon HCB surface concentration pointing to the radiation-induced catalytic activity of the alumina support. This is contrasted by experiments that were performed using the noncatalytic support, KBr, upon which no degradation was observed. The surface reactions were probed by FTIR-DR, UV-DR, GC-ECD, and GC-MS techniques. All results were consistent with the reductive dechlorination of HCB even though experiments were performed in an open atmosphere environment. Color centers were detected by FTIR and UV-DR in both KBr and alumina samples as well. In alumina samples, it is postulated that color centers (triplet excitons) may be reacting with surface hydroxyl groups to generate hydrogen atoms, essential for the reductive dechlorination of HCB. The dechlorination of HCB by direct electron transfer and/or hydrogen atom addition is proposed as the likely mechanisms of HCB degradation. This research suggests that the presence of oxides, alumina in particular, may accelerate radiolysis in heterogeneous or solid systems.

Acknowledgment. G.A.Z. would like to thank Dr. Deanna Hurum for her assistance in the analysis of FTIR data. K.A.G. gratefully acknowledges the support of the Occidental Chemical Corporation and the NSF (BES-9796058). P.V.K. acknowledges the support of the Office of Basic Energy Sciences of the Department of Energy. This is Contribution No. NDRL-4076 from the Notre Dame Radiation Laboratory.

References and Notes

(1) Hannay, N. B. *Semiconductors*; Reinhold Publ. Corp.: New York, 1959; p 54.
(2) Caffrey, J. J. M.; Allen, A. O. *J. Phys. Chem.* **1958**, *62*, 33−37.
(3) Wong, P. K.; Willard, J. E. *J. Phys. Chem.* **1969**, *73*, 2226.
(4) Wong, P. K.; Allen, A. O. *J. Phys. Chem.* **1970**, *74*, 774−778.
(5) Hentz, R. R.; Perkey, L. M.; Williams, R. H. *J. Phys. Chem.* **1966**, *70*, 731−735.
(6) Thomas, J. K. *Chem. Rev.* **1993**, *93*, 301−20.
(7) Linsebigler, A. L.; Lu, G.; Yates, J. T. **1995**, *95* (3), 735−758.
(8) Rojo, E. A.; Hentz, R. R. *J. Phys. Chem.* **1966**, *70*, 2919.
(9) Shkrob, I. A.; Trifunac, A. D. *J. Chem. Phys.* **1997**, *107*, 2374−2385.
(10) Su, Y.; Wang, Y.; Daschbach, J. L.; Fryberger, T. B.; Henderson, M. A.; Janata, J.; Peden, C. H. F. *J. Adv. Oxid. Technol.* **1998**, *3* (1), 63−69.
(11) Liu, D.; Kamat, P. V. *Langmuir* **1996**, *12* (9), 2190−2195.
(12) Lawler, A. *Science* **1997**, *275*, 1730.
(13) Schatz, T.; Cook, A. R.; Meisel, D. *J. Phys. Chem. B* **1998**, *102* (37), 7225−7230.
(14) Gray, K. A.; Clelland, M. R. *J. Adv. Ox. Technol.* **1998**, *3* (1), 22−36.
(15) Hilarides, R. J.; Gray, K. A.; Guzzetta, J.; Cortelluchi, N.; Sommer, C. *Water Environ. Res.* **1996**, *68* (2), 178−187.
(16) Hilarides, R. J.; Gray, K. A.; Guzzetta, J.; Cortellucci, N.; Sommer, C. *Env. Sci. Technol.* **1994**, *28* (13), 2249−2258.
(17) Buser, H. R.; Zehnder, H. J. *Experientia* **1985**, *41*, 1082−1084.
(18) Singh, A.; Kremers, W.; Smalley, P.; Bennett, G. S. *Rad. Phys. Chem.* **1985**, *25* (1−3), 11−19.
(19) Zacheis, G. A.; Gray, K. A. *Environ. Sci. Technol.*, submitted.
(20) Sparks, D. L. *Environmental Soil Chemistry*; Academic Press: New York, 1995; pp 39−40.
(21) Gebhart, R. E.; Lundgren, R. E. *Hanford Tank Clean up: A Guide to Understanding the Technical Issues*; Pacific Northwest National Laboratory Report (PNL-10773); Northwest National Laboratory: 1995.
(22) Stafford, U.; Gray, K. A.; Kamat, P. V.; Varma, A. *Chem. Phys. Lett.* **1993**, *204* (1), 55−61.
(23) Silverstein, R. M.; Bassler, G. C.; Morrill, T. C. *Spectrometric Identification of Organic Compounds*; John Wiley & Sons: New York, 1991; p 310.
(24) Oelkrug, D., Reich, S. *J. Phys. Chem.* **1991**, *95*, 269−274.
(25) NIST Standard Reference Data Program, Sadtler Research Labs − EPA Vapor Library, Gaithersburgh, MD.
(26) Nakanishi, K., Solomon, P. H. *Infrared Absorption Spectroscopy*; Holden-Day, Inc.: San Francisco, CA, 1977; p 12.
(27) Parkyns, N. D. *J. Chem. Soc. A* **1969**, 410.
(28) Frueh, A. J.; Golightly, J. P. *Can. Miner.* **1967**, *9*, 51.
(29) Serna, C. J.; White, J. L.; Hem, S. L. *Clays Clay Miner.* **1977**, *25*, 384.
(30) Garcia, J. V.; Ramas, C. J. *N. Jb. Miner Mh* **1987**, 397.
(31) Lee, D. H.; Condrate, R. A. *Mater. Lett.* **1995**, 241−246.
(32) Shafeev, G. A. *Adv. Mater. Opt. and Elect.* **1993**, *2*, 183.
(33) Agullo-Lopez, F.; Catlow, G. R. A.; Townsend, P. D. *Point Defects in Materials*; Academic Press: New York, 1988; pp 149−178.
(34) Rigole, M.; Depecker, C.; Wrobel, G.; Guelton, M.; Bonnelle, J. P. *J. Phys. Chem.* **1990**, *94*, 6743−6748.
(35) Anderson, J. H.; Lombardi, J.; Hair, M. L. *J. Colloid Interface Sci.* **1975**, *50*, 519.
(36) Pohle, W. J. *Chem Soc., Faraday Trans.* **1992**, *78*, 2101.
(37) Kendall, D. *Applied Infrared Spectroscopy*; Reinhold Publishing: New York, 1966; p 525.
(38) Skoog, D. A., Leary, J. J. *Principles of Instrumental Analysis*; Saunders College Publishing: Philadelphia, 1992; p 153.
(39) Schulman, J. H.; Compton, W. D. *Color Centers in Solids*, Pergamon Press: New York, 1962.
(40) Parker, J. H. *Phys. Rev.* **1961**, *124*, 703.
(41) Farhataziz, Rodgers, M. A. J. *Radiation Chemistry: Principles and Applications*, VCH Publishers, Inc.: New York, 1987; p 436−442.
(42) Mabuchi, T. *J. Phys. Soc. Jpn.* **1990**, *59* (2), 649−656.
(43) Suchet, J. D. *Crystal Chemistry and Semiconductivity in Transition Metal Binary Compounds*; Academic Press: New York, 1971; p 63.
(44) Vinodgopal, K.; Kamat, P. V. *J. Phys. Chem.* **1992**, *96*, 5053−5059.
(45) Wang, M.-J.; Jones, K. C. *Chemoshpere*. **1991**, *23* (5), 677−691.
(46) Cunningham, G.; Al-Sayyed, G.; Srijaranai, S. *Aquatic and Surface Photochemistry*; Lewis: Boca Raton, 1994; p 317−346.
(47) Torrents, A.; Stone, A. T. *Environ. Sci. Technol.* **1991**, *25*, 143−149.
(48) Fendler, E. J.; Fendler, J. H. *Prog. Phys. Org. Chem.* **1970**, *7*, 229−335.
(49) Zhang, G. H.; Mao, Y.; Thomas, J. K. *J. Phys. Chem. B* **1997**, *101*, 7100−13.
(50) Itoh, C.; Tanimura, K.; Itoh N. *J. Phys. C* **1988**, *21*, 4693.
(51) Choi, W.; Hoffmann, M. R. *Environ. Sci. Technol*. **1995**, *29* (6), 1646−1654.
(52) Terzian, R.; Serpone, N.; Draper, R. B.; Fox, M. A.; Pelizzetti, E. *Langmuir* **1991**, *7* (12), 3081−3089.